On the robustness of species coexistence to environmental perturbations

Mario Desallais[1], Michel Loreau[1,2], & Jean-François Arnoldi[1]

[1] Station d'écologie théorique et expérimentale (SETE), Centre National de la Recherche Scientifique – Moulis, France
[2] Institute of Ecology, College of Urban and Environmental Sciences, Peking University – Beijing, China

Correspondence: mario.desallais@sete.cnrs.fr

Abstract

Here we examine how biotic interactions determine the robustness of species coexistence in the face of environmental perturbations. For Lotka-Volterra community models, given a set of biotic interactions, recent approaches have characterized, and applied, the probability of finding at set of species intrinsic features (e.g. intrinsic growth rates) that will allow coexistence. Here we ask instead: if species do coexist, given their interactions, how fragile this coexistence should be to variations in species demographic parameters ? This change of framing allows us to derive the essential features of interactions that determine the robustness of coexistence, while not reducing it to a single number. As we illustrate on data from experimental plant community experiments, our results generate new ways to study species' contextual role in maintaining coexistence, and allows us to quantify the extent to which species intrinsic features and biotic interactions favourably combine (making coexistence more robust than expected), or oppose (making coexistence less robust than expected). Because it has both as central tenets, our work helps synthesize coexistence and ecological stability theories.

Keywords: Community; Perturbation; Stability; Feasibility domain; Persistence

Introduction

Understanding why and how species coexist is a central question in community ecology (Armstrong and McGehee, 1976; Chesson, 2000; Hastings, 1980; Hutchinson, 1961). Many studies have focused on what makes coexistence possible, and in particular on the role of the network of interactions between species (Abrams, 1984; Abrams et al., 2003; Brose et al., 2006; Otto et al., 2007; Williams, 2008). In the context of Lotka-Volterra models (the simplest mathematical representations of the population dynamics of interacting species), to quantify the role played by biotic interactions in species coexistence, a recent and growing body of theoretical work proposes to study the volume of a community's so called 'feasibility domain' (Rohr, Saavedra, and Bascompte, 2014; Rohr, Saavedra, Peralta, et al., 2016; Saavedra et al., 2017; Song, Rohr, et al., 2018). Given the set of biotic interactions between species, this feasibility domain is defined as the range of species intrinsic features (thought to reflect abiotic conditions that do not depend on the presence of the other species considered, such as intrinsic growth rates or carrying capacities) that allow species to coexist (Fig. 1). The idea here is that the larger this domain, the more likely a community is to withstand environmental disturbances while maintaining coexistence (Bartomeus et al., 2021; Song, Altermatt, et al., 2018).

However, the fact that a large set of conditions allows coexistence does not necessarily mean that coexistence is robust to environmental change. This can be visualized geometrically: a thin elongated feasibility domain could have a large volume, yet only contain fragile coexistence states, vulnerable to small changes in abiotic conditions. This observation reflects the tenuous distinction between two seemingly equivalent questions: "how likely will species coexist?", whose answer, in L-V models, corresponds to the size of the feasibility domain, and "If species do coexist, how fragile will this coexistence be?". This difference between raw and conditional probabilities of coexistence has led to the emergence of shape metrics of feasibility domains (Grilli et al., 2017; Saavedra et al., 2017). Recently Allen-Perkins et al. (2023) showed that a notion of 'domain asymmetry' can be correlated with variations of population dynamics across species in experimental plant-communities. These results are promising, but do not yet test quantitative predictions regarding the robustness of species coexistence to actual perturbations. They show that theoretical rankings of species vulnerabilities, based on the shape of the feasibility domain, are consistent with observed variations in population dynamics. Here, to make feasibility theory more directly interpretable, we will include ecological perturbations in its formulation. The goal would then be to move beyond a purely geometric description of the feasibility domain, and explicitly characterize the robustness of coexistence to environmental perturbations.

We will model ecological perturbations as long term changes species intrinsic features (such as their growth rates or carrying capacities) and derive, for any realized coexistence state, a notion of distance to the edge of feasibility: the minimal environmental perturbation intensity z able to lead at least one species to extinction. Our goal is to determine, amongst all coexistence states, the proportion $p(z)$ that lie within distance z from the edge of feasibility. For a given feasibility domain, this function $z \mapsto p(z)$ describes the distribution of distances to its edges, thus characterizing both the size and shape of the domain. If function $p(z)$ rapidly grows towards 1 this means that coexistence is typically fragile. In fact, function $p(z)$ allows quantifying the interrelation between intrinsic features of species and their interactions. If in a given state, $p(z)$ is close to 1, this means that in this environment, species intrinsic features and biotic interactions combine favourably. Our mathematical analysis aims to find the essential features of the function $p(z)$ that can be computed from the matrix of biotic interactions.

We then apply our methods to data from experimental plant community experiments (Van Ruijven and Berendse (2009) analyzed by Barbier et al. (2021), who computed the carrying capacities and interaction forces of species). This analysis reveals the role played by the various plant species in maintaining coexistence, which we relate to the degree of facilitation or competition experienced by each species. We also quantify the adequacy, in terms of coexistence, between biotic and abiotic conditions in those plant communities. The goal

here is to make a proof of concept, demonstrating a theoretical method for future experiments aimed at characterizing a particular type of environment and how well it matches a particular assemblage of species in terms of maintaining coexistence. Overall, considering the ease of computation of our metrics and the several novel application that emerges from them, our work should facilitate the use of this feasibility theory for experimental purposes (Allen-Perkins et al., 2023; Song, Simmons, et al., 2023; Wainwright et al., 2018)

Figure 1. The feasibility domain $D_f(A)$ (in light red on the left) is defined as the subset of growth rate directions that, given a pair-wise interaction matrix A, allows coexistence between all species. It is the intersection of the sphere with the image in r-space (via the matrix A) of the positive quadrant in N-space (shown on the right). The shape and volume of the feasibility domain corresponds to the shape and volume of the light red surface on the left. The probability of feasibility $\mathbb{P}(D_f)$ is the ratio between the volume of D_f and the volume of the unit sphere.

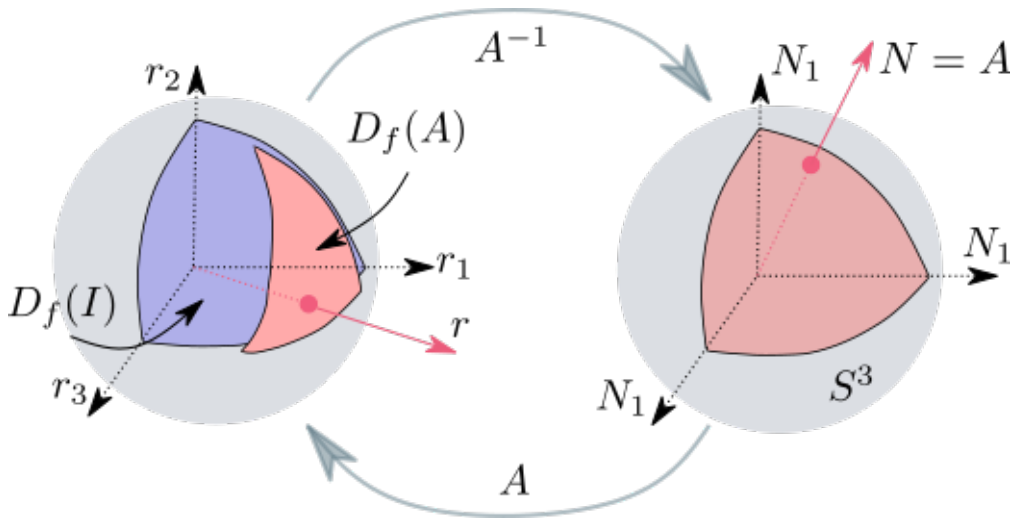

The feasibility domain

Consider a community of S species. Let N_i define the abundance of species i and r_i its intrinsic growth rate (which could be negative if the species cannot establish on its own), which encodes the effect of the environment on the ability of the species to grow if it were alone (Coulson et al., 2017; Levins, 1968; Meszéna et al., 2006; Roughgarden, 1975). The central object of study of feasibility is the matrix $A = (A_{ij})$ of pairwise biotic interactions between all S species in the community. A_{ij} encodes how a change in the abundance of species j, impacts the growth of species i. This can represent competition or facilitation depending on the sign of A_{ij}. The diagonal terms A_{ii} represent intraspecific competition, and will be assumed non-zero in our analysis. The generalized Lotka-Volterra (L-V) model prescribes the population dynamics of all species as (Volterra, 1926) :

$$\frac{dN_i}{dt} = N_i \cdot \left(r_i - \sum_{j=1}^{S} A_{ij} N_j \right) \quad \text{for } i = 1, \ldots, S \tag{1}$$

A growth rate vector $r = (r_i)$ is 'feasible' if the fixed point $N^*(r) = A^{-1}r$ of the above model is strictly positive, meaning that $N^*(r)_i > 0$ for all i. To consider the feasibility domain, we artificially assume that variations in growth rates are the result of a variation in abiotic conditions impacting the ability of species to grow on their own, but not their interactions (but see discussion). This abstraction leads to a definition of the feasibility domain associated with the interaction matrix A (Rohr, Saavedra, and Bascompte, 2014): the set of growth rate vectors $D_f(A)$ such that the equilibrium abundances are non zero. However, in the L-V model, multiplying all growth rates by a constant does not change coexistence. Thus the feasibility domain has to be defined as a set of *directions*, isomorphic to a solid angle in the r-vector space (Ribando, 2006; Saavedra et al.,

2017; Song, Rohr, et al., 2018), so a convex subset of the sphere (Fig. 1):

$$D_f(A) = \{r/||r|| \mid \text{such that } N^* = A^{-1}r \text{ is strictly positive}\} \tag{2}$$

We can also think of the relative volume of the domain as the probability of randomly drawing growth rates r which lead to positive abundances (Grilli et al., 2017). The random sampling must be though of as uniform in the space of growth rate *directions*. Importantly, drawing each species' growth rate r_i independently from a standard Gaussian distribution yields such a uniform sampling of growth rate directions. This remark, followed by the linear change of variables $A^{-1} : r \mapsto N$ then leads to the following formula for the relative volume of the feasibility domain :

$$\mathbf{P}(D_f) = \frac{1}{\sqrt{2\pi}^S} \int_{r \in D_f} e^{-\frac{||r||^2}{2}} d^S r = \frac{|A|}{\sqrt{2\pi}^S} \int_{\mathbf{R}_+^S} e^{-\frac{||AN||^2}{2}} d^S N \tag{3}$$

$\mathbf{P}(D_f)$ is thus the cumulative distribution, noted $\Phi_{A^\top A}(0)$, of a multivariate normal distribution centered on 0 and with covariance matrix $C = (A^\top A)^{-1}$. In the absence of interactions $\mathbb{P}(D_f) = 2^{-S}$. To focus on the effect of interactions it is thus convenient to define a ratio of probabilities Saavedra et al. (2017):

$$\Omega(A^\top A) = 2^S \cdot \Phi_{A^\top A}(0) \tag{4}$$

Within this formalism, Ω corresponds to the effect of species interactions on the probability of coexistence and is equal to 1 in the non-interaction case.

Distribution of distances to the edge of feasibility

If a community of species is in a state of stable coexistence, how difficult is it for it to lose coexistence? In other words, what is the minimum disturbance that a community can experience without leaving the feasibility domain? This depends on how close to the boundary the growth rate vector was in the first place and can correspond to the 'robustness' or the 'full resistance' notion that was defined recently in Lepori et al. (2022) and Medeiros et al. (2021). Here we want to go beyond the characterization of a given realized community, i.e. its distance from the edge of feasibility, and understand the contribution of the interaction network to the robustness integrated over all possible communities. This will allow us to isolate the role of species interactions, but also to determine the degree to which an actual growth rate vector favours coexistence: given the interactions, is this vector particularly close or far form the edge of the feasibility domain?

Distribution of distances from the edge in standard triangles

If the community is made of three species, the feasibility domain corresponds to a solid angle, which defines a triangle drawn on a sphere (see Fig. 1). We thus start with a simplified analysis of regular triangles. This analogy allows us to gradually introduce the logic behind our geometrical approach (see Fig. 2). In this detour into simple trigonometry, which may seem removed from the initial ecological question, we will create a shape metric capable of encapsulating all the subtleties of shape differences between triangles (see Fig. 2).

The probability of a point to be at a distance greater than z from one of the triangle's edges corresponds to the relative area of the inscribed triangle whose own edges are exactly at a distance z from the boundaries of the original one (see the left panel of Fig. 2). Knowing A, the area of the original triangle, and A', the area of the inscribed triangle, the proportion $p(z)$ of points that lie within a distance z from an edge is thus $p(z) = \dfrac{A - A'}{A}$. If P is the perimeter of the original triangle, it is an easy exercise to show that

$$p(z) = 1 - \left(1 - \frac{z}{D_*}\right)^2$$

In this expression, $p(z)$ is fully parameterized by the number $D_* = 2A/P$, which is the radius of the largest disc contained in the triangle (we can verify that $p(D_*) = 1$). At fixed perimeter P, the larger D_* is, the larger

Figure 2. Left: Triangles are parameterized by their base l, height h, and perimeter P. Their area is $A = h\ell/2$, and we are interested in the fraction $p(z)$ of points that lie within a distance z from an edge. We can show that $p(z) = 1 - (1 - z/D_*)^2$ which is fully parameterized by $D_* = 2A/P$, the radius of the inscribed disc, whose center is equidistant to all edges of the triangle. Right: at a fixed area A, D_* grows as triangles approach an equilateral triangle (which minimizes the perimeter P).

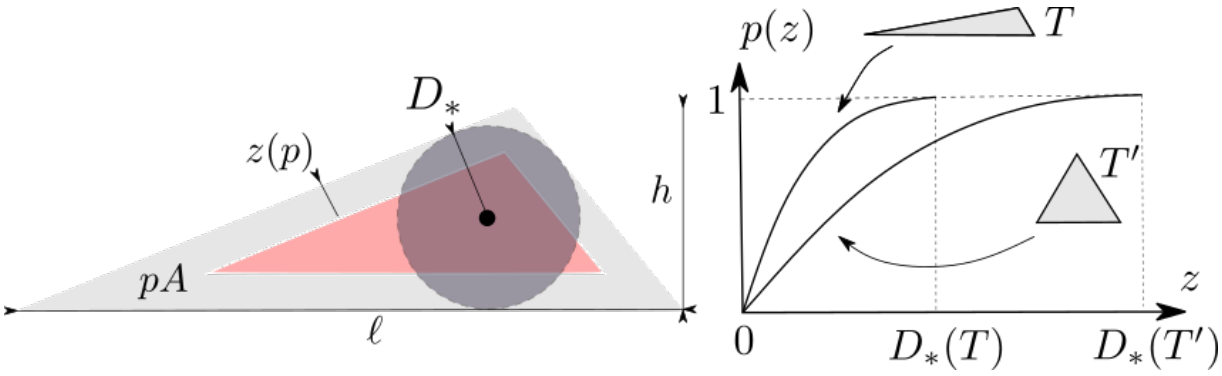

this distance, and thus the 'bulkier' the triangle is. As expected, D_* is maximal for equilateral triangles, which for a fixed perimeter, maximize the area. This single distance measure D_* therefore allows us to quantitatively express differences in shape and size between triangles, and quantify, via the function $p(z)$ above, the relative positioning of a given point within a triangle. For instance, If $p(z) > 0.5$, this point is further from the edges than most. In the next sections we will show how we come to interpret such a situation as a case where, given the interaction network, the growth rate of species favour robust coexistence. But before we can make such ecological interpretations, two steps remain. First, we must show that the distance z is a measure of the intensity of environmental disturbances able to push species to extinction. Second, we need to generalize our geometrical ideas to feasibility domains, that are not simple triangles, and can be of any dimension (i.e. any number of species).

Perturbation intensity as a distance to the edge of feasibility

We consider a perturbation as a change in environmental conditions that occurs on a long-time scale, modeled as a variation $\delta r = (\delta r_i)$ of species intrinsic growth rates. In L-V models, this will eventually lead to a shift of abundance of any species i:

$$N_i(r + \delta r) - N_i(r) = \sum_j (A^{-1})_{ij} \delta r_j = \langle v^{(i)}, \delta r \rangle \tag{5}$$

where the vector $v^{(i)}$ is the ith row of the inverse interaction matrix A^{-1}. The vector $v^{(i)}$ thus encodes the species sensitivity to environmental perturbations (Bender et al., 1984). To lose coexistence, the perturbation must lead to the extinction of at least one species. This implies that $|\langle v^{(i)}, \delta r \rangle|$ is equal to N_i^* for some species i. The minimal disturbance intensity (the norm of the vector δr) able to cause an extinction gives us a notion of distance to the edge of the feasibility domain. Given that $|\langle v^{(i)}, \delta r \rangle| \leq ||v^i|| \times ||\delta r||$, this distance is:

$$z = \min_i \frac{N_i(r)}{||v^i||} \tag{6}$$

This value depends linearly on the norm of r (via the term $N_i(r)$). To standardize distances, we impose that $||r||^2 = S$. We will soon see why this choice is a natural one.

The most robust state of coexistence and the radius D_* of the inscribed disc

Here we look for the maximal distance to the edge of feasibility. To do so we fist locate the incenter r^c of the domain, and its distance D_* to the edge. The incenter is equidistant to all edges, meaning that $\frac{N_i^c(r^c)}{||v^i||} = D_*$ for all i. Thus, using the fact that $AN^c = r^c$, and introducing the vector of maximal sensitivities $v = (||v^i||)$, we get that

$$r^c = D_* \times Av \tag{7}$$

The value of D_* follows from the normalization of growth rates (i.e. $||r^c||^2 = S$). We then deduce that

$$D_* = \frac{\sqrt{S}}{||Av||} \tag{8}$$

In the absence of interactions, and thus when A is diagonal, we have $D_* = 1$. This is what justifies our choice of growth rate normalization. For regular triangles, this maximal distance was the sole parameter of the function $p(z)$ that describes the proportion of points within a distance z to an edge. In the case of feasibility domains, all we know at this point is that $p(D_*) = 1$. This makes D_* a natural characteristic distance, to which the intensity of any environmental perturbation should be compared. However, we will see in the next section that the raw number of species S also plays a crucial role, as well as a different quantity, very much related to D_*, that controls the behavior of $p(z)$ for small z values.

Edge effects in high dimensions, and the role of species richness

Above we focused on the largest distance to an edge of the feasibility domain where $p(z) = 1$. Now we want to understand the initial behavior of $p(z)$ and therefore, small z distances. To do so, we use the Gaussian integral characterization of the feasibility domain. Using the Gaussian cumulative function $\Phi_{A^\top A}$ defined in section 1 that follows from the change of variables $r \to N$, the proportion of feasible growth rate vectors that lie within a distance z from an edge can be calculated as

$$p(z) \approx 1 - \frac{\Phi_{A^\top A}(-zv)}{\Phi_{A^\top A}(0)} \tag{9}$$

where $v = (||v^i||)$ is the vector of maximal species sensitivities. The argument $-zv$ in the cumulative function means that we integrate over growth rate vectors r such that the corresponding abundances N_i are larger than zv_i. The. approximation comes from the fact that the growth rate vectors r are only normalized on average (i.e. $\mathbb{E}||r||^2 = S$). However, this has negligible effects for S large enough (i.e. in high dimensions). This approximation is crucial to keep mathematical tractability. By differentiating $p(z)$ at $z = 0$ we get the initial behavior of $p(z)$, which describes the edge of feasibility. This derivation is relatively simple to carry out and gives

$$p'(0) = S\sqrt{\frac{2}{\pi}} \times \frac{1}{S}\sum_{i=1}^{S} v_i \sqrt{\frac{|A^\top A|}{|(A^\top A)_{/i}|}} \frac{\Omega_{/i}}{\Omega}$$

In this expression, a matrix $B_{/i}$ is one where the ith row and column have been removed. $\Omega = 2^S \Phi_{A^\top A}(0)$ is the rescaled volume of the feasibility domain, while $\Omega_{/i} = 2^{S-1}\Phi_{(A^\top A)_{/i}}(0)$ is essentially the rescaled volume of the feasibility domain in the absence of species i. This leads us to define

$$D = 1/\frac{1}{S}\sum_{i=1}^{S} v_i \sqrt{\frac{|A^\top A|}{|A^\top A|_{/i}}} \frac{\Omega_{/i}}{\Omega} \tag{10}$$

which is equal to 1 in the absence of interactions. The expression for D is quite different (and more complicated) to the expression for maximal distance D_*. Nonetheless those two distances are closely related and take very similar values, with $D \approx D_*$ for the vast majority of random interactions matrices that we generated, and even more so when considering empirically inferred matrices (See 7 in Supplementary material).

Distribution of distances from the edge for general feasibility domains

So now we have $p(z) \approx S\sqrt{\frac{2}{\pi}} \times \frac{z}{D}$ when z is small, while in the previous section we had $p(z = D_*) = 1$. This leads us to a simple approximation that mimics the regular triangular formula for the distribution of distances in the feasibility domain (see Fig. 3 for a numerical example)

$$p(z) \approx 1 - (1 - \frac{z}{D_*})^{S\sqrt{\frac{2}{\pi}}\frac{D_*}{D}} \tag{11}$$

There are thus two characteristic distances: D_*, which does not explicitly depend on S, and $D/S\sqrt{\frac{2}{\pi}}$, which decays rapidly with species richness. The latter behavior occurs because when there are many species present, it is ever more likely that one of them is close to local extinction. This diversity effect will tend to take a dominant part in shaping the function $p(z)$. Geometrically speaking, this effect comes from the fact that in high dimensions, even very thin neighbourhoods of the edge of a closed object will cover a dominant fraction of the overall volume of that object [1].

Figure 3. Left : empirical distribution of distances $p(z)$ for a random interaction matrix between $S = 6$ species, compared with its analytical approximations (equations 9 and 11). The simplest expression, which constitutes our main result, is the one given in equation 11, shown in orange. On the other hand, as the number of species S increases, the approximation based of equation 9, shown in green, becomes more and more accurate. Right: comparison the two approximations (equations 9 and 11) for 100 randomly drawn $S \times S$ interaction matrices and growth rate vectors (each point is one matrix and one growth rate vector, so one value of z). We chose S between $S = 3$ and $S = 10$, with a variety of connectance values, pairwise interaction strengths, as well as a variety of values for diagonal elements, which represent different scenarios of self-interaction.

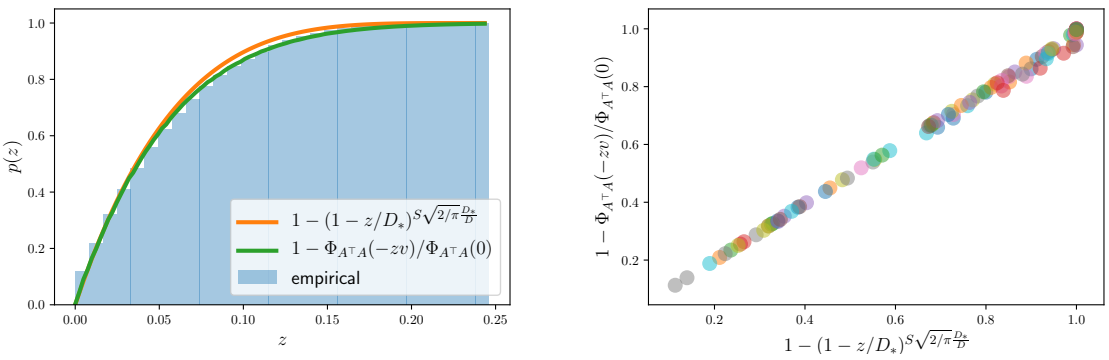

Contextual species contributions to the robustness of coexistence

The above analyses of the distribution of distances to the edge of feasibility enable us to characterize the robustness of coexistence of an ecological community. Further, the two distances D and D_* that parameterise this distribution can allow us to describe the contributions and contextual roles of species.

To see this, let us first go back to the derivation of D_* which is the distance to the edge of feasibility of the most robust state, i.e. the incenter of the domain. Note that

$$r_i^c/D_* = \sum_j A_{ij} v_j \tag{12}$$

is a measure of the strength of competition exerted by the community on species i. It represents the sum of interactions felt by that species, but where each per-capita interaction term A_{ij} is weighted by the partner's

[1] This can be seen by rescaling distances as $\hat{z} = S\sqrt{\frac{2}{\pi}} \times z$, and take the limit of large S. Our ansatz above indeed becomes $p(\hat{z}) \approx 1 - e^{-\hat{z}/D}$ where the influence of the larger distance D_* has dissolved into irrelevant asymptotic behaviour.

maximal sensitivity to perturbations (the terms v_j). A weak interaction with a highly sensitive species (a large v_j) can thus contribute more than a weak interaction with a highly stable population (a small v_j). If $r_i^c/D_* = 1$, the community has a neutral effect, equal to that of the species on its own. If it is less than 1, the community facilitates that species (see Fig. 8). We will use this interpretation in the last section to assess the individual positioning of species in determining the robustness of coexistence (see Fig. 4).

We now turn our attention to D, which describes the shape of feasibility domain near its edges. It consists of an average of S elements, one for each species i. Those elements relate to the individual vulnerability of each species. Indeed, they determine the distribution of coexistence states for which that each species is within a certain pertubation distance from extinction. We can thus use the expression of D to quantify the species vulnerability to perturbation, given coexistence (SCV):

$$(\text{SCV}_i) = v_i \sqrt{\frac{|A^\top A|}{|A^\top A|_{/i}} \frac{\Omega_{/i}}{\Omega}} \tag{13}$$

We can thus conduct our analysis of the robustness of coexistence at the species level, rather than solely at the level of the entire community. To understand the role of each species, we can correlate their relative SCV$_i$ values with how hostile the community is to the species, as measured by relative r_i^c/D_* values (see Fig. 4). Intuitively, the two should be strongly correlated: species that perceive a hostile biotic environment should also be the most vulnerable, and vice versa. But this need not always be so simple. If a species is itself very hostile towards an otherwise relatively favourable community, the coexistence of all species would require this hostile species to be vulnerable, as coexistence would only be possible in abiotic environments unfavourable to it. By contrast, a species to which the community is relatively hostile could nonetheless be relatively robust if its persistence at high enough densities is required for the persistence of other species. Here those various qualitative roles clearly depend on the biotic context. The same species could change roles depending of which community it is part of.

Application to data from a grassland experiment

Our approach enables us to characterize the robustness of coexistence at two levels: at the scale of the community as a whole, but also at the species scale. Here, we illustrate the insights that this approach can generate for real ecological communities. We revisite data from Van Ruijven and Berendse (2009) and its subsequent analysis by Barbier et al. (2021), compiled from long-term studies of plant communities in the experimental gardens of Wageningen University, Netherlands. Here we directly use the results of Barbier et al. (2021), who estimated the interaction strengths between 8 plant species, as well as their carrying capacities. Interations refer here to a Lotka-Volterra parametrization that differs from the one that implicitly follows from equation 1. Indeed, monocultures where used to infer species' carrying capacities K_i, and it is those that we consider as proxys for the abiotic conditions (and not intrinsic growth rates r_i). The relevant interaction matrix, inferred using duo-culture experiments, follows from re-writing the L-V equations as

$$\frac{dN_i}{dt} = \frac{r_i N_i}{K_i} \left(K_i - \sum_j A_{ij} N_j \right) \tag{14}$$

In this parametrization, A_{ij} has no dimensions and satisfies $A_{ii} \equiv 1$. On the basis of pairwise interaction values, we then reconstruct interaction matrices consisting of 4 species, which have been experimentally realized (Van Ruijven and Berendse, 2009).

To show the role of the same species in different communities, we calculated SCV$_i$ and r_i^c/D_* for each species within all four-species communities (See left panel of Fig. 4). We normalized these values by the mean value within each community to obtain relative species contributions to vulnerability and relative biotic effects on species, as the same species can hold different roles for the robustness of coexistence, depending

on the biotic environment. Furthermore, while we unsurprisingly find the same trend as in Fig. 8 (The majority of points being located in the red and green areas and being either "Highly Competitively Constrained and Vulnerable" or "Less Competitively Constrained and Robust"), we can observe non-trivial cases (blue areas of the figure). In these cases, the biotic interactions affecting the species in question are not sufficient to explain its contribution to vulnerability.

The "Less Competitively Constrained yet Vulnerable" points correspond to a case where the strong contribution of each species to vulnerability comes from its competitive forces applied to other species. Indeed, to achieve coexistence, it must necessarily be of low abundance and therefore vulnerable, so that other species do not suffer too greatly from its presence. The "High Competitively Constrained yet Robust" points correspond to the case where species are useful for the coexistence of others and therefore have a high abundance (and a low contribution to the vulnerability of coexistence) despite higher competitive forces experienced. These non-trivial cases explain why some points in Fig. 8 deviate from the observed correlation.

Figure 4. Analysis of the robustness of coexistence at the species scales. Each point on the left graph represents all the individual positions of the 8 species of the dataset within the 35 possible 4-species communities where they are present. On the x-axis, the relative effect of interactions (biotic environment) is indicated (r_i^c/D^* divided by the mean value for all species). On the y-axis, the relative contribution to the vulnerability of each species is indicated (SCV$_i$, divided by the average on all species). This allows us to define 4 notable cases, represented on the graph on the right by the different colors.

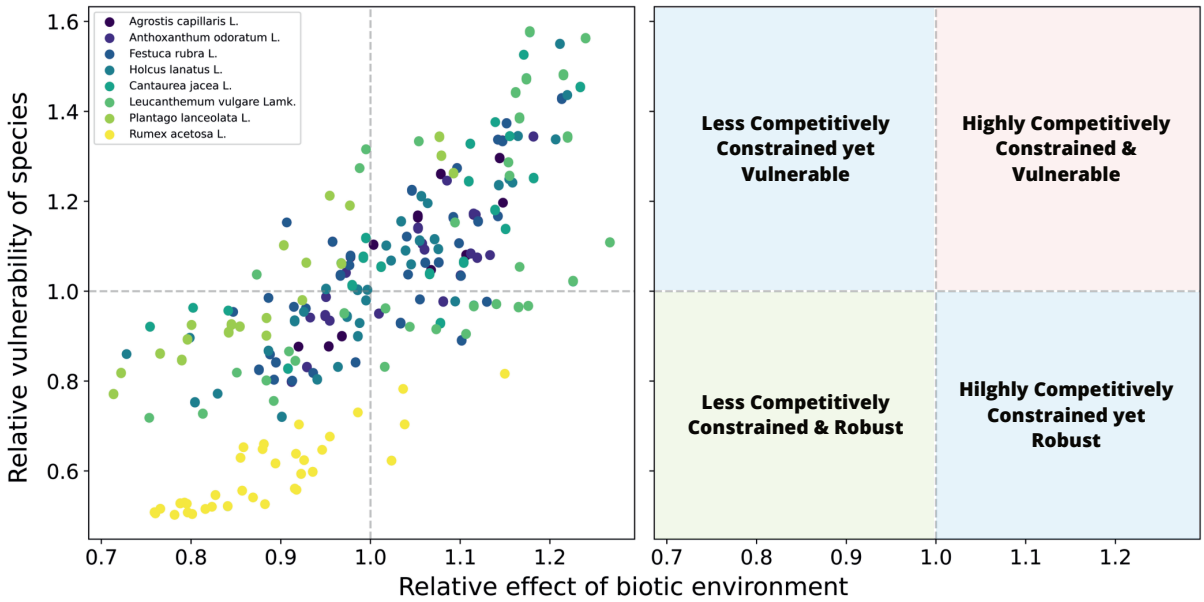

Interestingly, the points cluster relatively well by species. This suggests that within the different 4-species communities formed by the 8 selected species, the species tend to maintain a relatively identical biotic role. Note that the abiotic environment in which these species have grown is supposedly the same. This makes ecological sense, as the biotic roles of each species depend on their phenotypic traits, and are therefore fixed by the biology of each species. For example, *Rumex Acetosa L.* is predominantly found in the green zone in Fig. 4, suggesting good persistence through low competitive forces. This fits rather well with its characterization as a weed species, present in a wide range of environments and able to coexist and persist within many ecosystems (Korpelainen and Pietiläinen, 2020).

In addition, since the abiotic environment was assumed to be the same in the experiment, we can characterize it and determine whether the particular realization of a community is subject to a match between interactions favoring the robustness of coexistence and an environment favorable to this same robustness. Indeed, using the carrying capacities determined during the experiments, we can precisely determine z_r, the

Figure 5. Using the empirically inferred interaction matrix between 8 plant species (Barbier et al., 2021) and their carrying capacities (taking median values for simplicity), we assembled all theoretically feasible 4-species communities (27 out of the 70 different combinations turn out to be feasible). Left: The interaction matrix for each community defines a curve, and the realized community gives the point on the curve. Large values of z_r (x-axis) implies high robustness (i.e. large distance from the edge of feasibility), whereas large values of $p(z_r)$ means that most communities with similar interactions are less robust (they are close to the incenter of the feasibility domain). The shape of the curves encodes the relevant shape and size attributes of the feasibility domain. Right: once rescaled by the characteristic distance D_*, all curves collapse on a single one, the graph of $p(z) = 1 - (1 - \frac{z}{D_*})^{S\sqrt{\frac{2}{\pi}}}$ (here $S = 4$). This is due to the fact that, for those interaction matrices, $D_* \approx D$ (see supplementary figure B.7).

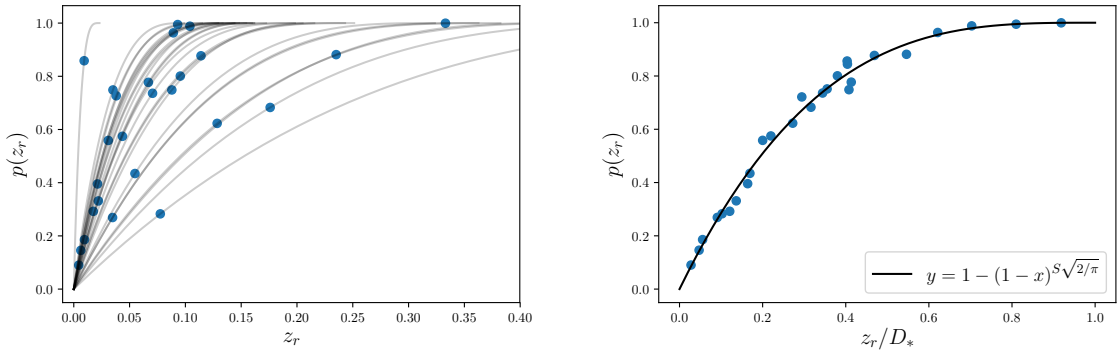

minimal distance to the edge of the realized community, and p(z_r), the proportion of points within this distance. This allows us to place all the communities on the z/D and $p(z)$ curve (see Fig. 5). If $p(z_r) = 1$ for a community, it means that in this environment, the realized community has the most advantageous combination of biotic interactions (interaction matrix A) and intrinsic species parameters (carrying capacity K), in terms of robustness of coexistence. If $p(z_r)$ is low for a certain community, it means that this environment has led to a kind of mismatch between species interactions and species growth rates, which therefore induces a low robustness of coexistence.

Discussion

For a given community of species, we focused on the function $p : z \mapsto p(z)$ that maps a value of environmental perturbation intensity z to the fraction of coexistence states from which coexistence can be lost following such perturbations. As it turns out, $p(z)$ is a rich object to study the robustness of species coexistence, and how biotic interactions affect it, while not reducing robustness to a single number.

In Lotka-Volterra models, the function $p : z \mapsto p(z)$ characterizes the shape of the feasibility domain – the set of growth rate vectors that allow stable coexistence between all species. Indeed, for a given feasibility domain, $p(z) = \mathbb{P}(dist \leq z)$ determines the distribution of distances to its edges (see Fig. 3). For a given coexistence state, the distance to an edge corresponds to the state's "robustness" or "full resistance", as defined by Lepori et al. (2022) and Medeiros et al. (2021). Any coexistence state is associated to a distance z to the edge of feasibility. The larger this distance, the more robust the state. The value of $p(z)$ tells us if this robustness is particularly high or low, given the set of biotic interactions. If $p(z)$ is close to 0 we can say that, in terms of maintaining coexistence, the set of species growth rates is not well aligned with the set of biotic interactions.

We showed that $p(z)$ is fully parameterized by two characteristic distances D and D_* defined so that they

are equal to 1 in the absence of interactions, as well as species richness S:

$$p(z) = 1 - (1 - \frac{z}{D_*})^{S\sqrt{\frac{2}{\pi}}\frac{D_*}{D}}$$

D_* is the maximal distance, the robustness of the most robust state, so that $p(z = D_*) = 1$. We derived a remarkably simple formula (see equation 8) for D_*, based on the interaction matrix and its inverse. Unpacking the expression for D_* also allowed us to give a species-level characterization that can be interpreted as measuring the effective amount of competition that any given species feels, where its interactions are weighted by the sensitivities of its interacting partners. The other important distance, D, once divided by S, determines the behaviour of $p(z)$ at small perturbation intensity values, thus describing the edges of feasibility, which take up most of its volume if S is large. This last remark is only a geometrical way of saying that for many interacting species, in the absence of prior knowledge of abiotic conditions, there is a high chance that at least one of those species is close to extinction. The expression for D (see equation 10) is less simple than the one for D_*, but can also be used to give a species-level characterization of coexistence. Indeed, as in Allen-Perkins et al. (2023), we can decompose D to measure the robustness of each species persistence conditioned on overall coexistence. This interpretation, together with the one relating D_* to effective competition pressure, can be used to reveal the contextual roles of species in maintaining coexistence. The biotic context created within a coexisting community can be favorable or unfavorable to individual species through the balance of interactions they receive and emit and how hostile they are to others (See different panels of Fig. 4).

We insist that it is remarkable that only two values computed from the set of biotic interactions are enough information to fully characterize the distribution of distances of the feasibility domain, as the latter gives a complete and multidimensional description of the robustness of coexistence under press perturbations.

Broadly speaking, our theory highlights a negative effect, amplified by species richness, of the intensity of the interaction forces and the sensitivity of the species on the robustness of coexistence. Figure 4 and 8 also show the relationship between strong inter-specific competition faced by species and their contribution to the vulnerability of coexistence. These results are consistent with the existing literature on the effect of interactions on community coexistence or stability under environmental perturbations (Barabás et al., 2016; Chesson, 2000; Hale et al., 2020; Mccann et al., 1998; Vallina and Le Quéré, 2011). The fact that features of the inverse interaction matrix are present in both D and D_* highlights the importance of network structure, as the inverse matrix encodes net effects between species, via all indirect interaction pathways. For the same overall mean interaction strength, net effects can be very different depending on the way the matrix A is organized. This is consistent with previous research on the effect of network structure on coexistence (especially in cases with more than two species) as on other stability notions (Barabás et al., 2016; Cenci et al., 2018; Lurgi et al., 2016; Serván et al., 2018). This leads to our major ecological conclusion: vulnerability to extinction depends on how a species is affected by others through direct interactions, combined with the sensitivities of those species (how they amplify environmental change). Here sensitivity is a potentially collective notion that arises from indirect interactions between species, and is thus sensitive to the interaction structure.

Unlike previous measures of asymmetry of the feasibility domain (See Appendix S7 of Grilli et al. (2017) and Saavedra et al. (2017) and later Tabi et al. (2020) and Allen-Perkins et al. (2023)), we included the notion of disturbance in the mathematical definition of z (see equations 5 and 6). It is this step that subsequently allows us to dispense with a purely geometric analysis of the feasibility domain, and instead use standard objects of the Lotka-Volterra model (the matrix A and its inverse, which commonly occur in stability analysis). However, our theory strongly depends on the way environmental disturbances are modeled. This highlights the importance of taking into account the type of disturbance when studying the stability of a community (Arnoldi, Bideault, et al., 2018; Arnoldi, Loreau, et al., 2019; Bender et al., 1984) and suggests that different results could be obtained by considering other types of disturbance (ie. that vary through time, and/or scale with species standing biomass). Deepening our theory to account for more general types of disturbance could

be an interesting direction.

It should be made clear that we did not directly test the relevance of our function $p \mapsto p(z)$ to predict actual species persistence under real environmental perturbations. To do so, we would need to compare these metrics on experimental datasets highlighting the persistence of species over time. This is precisely what Allen-Perkins et al. (2023) have done, and their "Asymmetry index" bares many similarities with our analysis (use of the incenter position, species-level contributions to coexistence). Their results show a good match between the species' actual persistence over time and the predictions made based on their indexes. Also, their recent measurement seems far less sensitive than others with small feasibility domains and large community sizes, and is therefore far more practical to use. We can see our analysis as an extension of theirs, and the results of their data analysis are a good indication that this extension relies on solid foundations, both theoretically and empirically, to study species coexistence and persistence.

Coexistence is defined as the maintenance of positive abundance of all species in a community. No attention is paid to total biomass, ecosystem functions, turnover, or processes at the meta-community level. Our results should therefore not be interpreted as evidence of a negative effect of biodiversity on stability in the sense of maintaining biomass or ecological function over time (Loreau and Mazancourt, 2013), nor on the resistance or resilience of the the community (Arnoldi, Loreau, et al., 2016; Kéfi et al., 2019). It simply highlights the difficulty for complex interaction networks to generate communities that can tolerate environmental disturbances without losing any species. This vision of a fixed community and coexistence seen as the absolute persistence of all species over time is, however, limiting and open to criticism. It would be interesting to develop approaches that include possible turnover or variations in the species pool over time.

Another caveat is the supposed independence between biotic and abiotic parameters. This unrealistic assumption means that a change in abiotic environmental conditions (disruption of growth rates or carrying capacity) should not change biotic interactions. This assumption is necessary to define the feasibility domain (Saavedra et al., 2017). However, the empirical applications we present (determination of the biotic role of different species within several communities; quantification of the adequation between a given abiotic environment and a certain biotic assemblage) illustrate how to overcome this issue. Indeed, in the experimental data, the abiotic environment is the same for each community studied and is not subject to change.

Overall, this study provides an understanding of the link between the conditions under which communities coexist and the robustness of this coexistence. On the one hand, the analytical results provide a clear explanation of the relationships between the various mathematical elements involved in feasibility domain analysis. On the other hand, they enable us to link the interpretations made specifically through the analysis of the notion of feasibility domain to more general notions of community ecology. In doing so, we have linked different measures of stability and placed the robustness of coexistence within the multidimensional concept of ecological stability (Donohue et al., 2016; Radchuk et al., 2019).

Acknowledgements

We thank Matthieu Barbier for the data provided and useful discussions. We also thank Rudolf Rohr and Nicolas Loeuille for inspiring discussions throughout the article writing process.

Fundings

This work was supported by the BIOSTASES Advanced Grant, funded by the European Research Council (ERC) under the European Union's Horizon 2020 research and innovation programme (666971).

Conflict of interest disclosure

The authors declare that they comply with the PCI rule of having no financial conflicts of interest in relation to the content of the article.

Data, script, code, and supplementary information availability

Data and codes are available online: https://doi.org/10.5281/zenodo.10534236 ; For more information on the dataset, please contact Barbier et al. (2021)

References

Abrams (1984). Variability in resource consumption rates and the coexistence of competing species. *Theoretical Population Biology* 25, 106–124. ISSN: 0040-5809. https://doi.org/https://doi.org/10.1016/0040-5809(84)90008-X.

Abrams, Brassil, and Holt (Sept. 2003). Dynamics and responses to mortality rates of competing predators undergoing predator–prey cycles. en. *Theoretical Population Biology* 64, 163–176. ISSN: 00405809. https://doi.org/10.1016/S0040-5809(03)00067-4.

Allen-Perkins A, D García-Callejas, I Bartomeus, and O Godoy (2023). Structural asymmetry in biotic interactions as a tool to understand and predict ecological persistence. *Ecology Letters* n/a. https://doi.org/https://doi.org/10.1111/ele.14291.

Armstrong RA and R McGehee (June 1976). Coexistence of species competing for shared resources. en. *Theoretical Population Biology* 9, 317–328. ISSN: 00405809. https://doi.org/10.1016/0040-5809(76)90051-4.

Arnoldi JF, M Loreau, and B Haegeman (Jan. 2016). Resilience, reactivity and variability: A mathematical comparison of ecological stability measures. en. *Journal of Theoretical Biology* 389, 47–59. ISSN: 00225193. https://doi.org/10.1016/j.jtbi.2015.10.012.

Arnoldi JF, A Bideault, M Loreau, and B Haegeman (Jan. 2018). How ecosystems recover from pulse perturbations: A theory of short- to long-term responses. *Journal of theoretical biology* 436, 79–92. ISSN: 0022-5193. https://doi.org/10.1016/j.jtbi.2017.10.003.

Arnoldi JF, M Loreau, and B Haegeman (Oct. 2019). The inherent multidimensionality of temporal variability: how common and rare species shape stability patterns. *Ecology letters* 22, 1557–1567. ISSN: 1461-023X. https://doi.org/10.1111/ele.13345.

Barabás G, M J. Michalska-Smith, and S Allesina (July 2016). The Effect of Intra- and Interspecific Competition on Coexistence in Multispecies Communities. *The American Naturalist* 188. Publisher: The University of Chicago Press, E1–E12. ISSN: 0003-0147. https://doi.org/10.1086/686901.

Barbier M, C de Mazancourt, M Loreau, and G Bunin (Jan. 2021). Fingerprints of High-Dimensional Coexistence in Complex Ecosystems. *Physical Review X* 11. Publisher: American Physical Society, 011009. https://doi.org/10.1103/PhysRevX.11.011009.

Bartomeus I, S Saavedra, RP Rohr, and O Godoy (Mar. 2021). Experimental evidence of the importance of multitrophic structure for species persistence. en. *Proceedings of the National Academy of Sciences* 118, e2023872118. ISSN: 0027-8424, 1091-6490. https://doi.org/10.1073/pnas.2023872118.

Bender EA, TJ Case, and ME Gilpin (Feb. 1984). Perturbation Experiments in Community Ecology: Theory and Practice. en. *Ecology* 65, 1–13. ISSN: 00129658. https://doi.org/10.2307/1939452.

Brose U, RJ Williams, and ND Martinez (Nov. 2006). Allometric scaling enhances stability in complex food webs. eng. *Ecology Letters* 9, 1228–1236. ISSN: 1461-0248. https://doi.org/10.1111/j.1461-0248.2006.00978.x.

Cenci S, C Song, and S Saavedra (2018). Rethinking the importance of the structure of ecological networks under an environment-dependent framework. en. *Ecology and Evolution* 8, 6852–6859. ISSN: 2045-7758. https://doi.org/10.1002/ece3.4252.

Chesson P (Nov. 2000). Mechanisms of Maintenance of Species Diversity. en. *Annual Review of Ecology and Systematics* 31, 343–366. ISSN: 0066-4162. https://doi.org/10.1146/annurev.ecolsys.31.1.343.

Coulson T, BE Kendall, J Barthold, F Plard, S Schindler, A Ozgul, and JM Gaillard (2017). Modeling Adaptive and Nonadaptive Responses of Populations to Environmental Change. *The American Naturalist* 190. PMID: 28829647, 313–336. https://doi.org/10.1086/692542. eprint: https://doi.org/10.1086/692542.

Donohue I, H Hillebrand, JM Montoya, OL Petchey, SL Pimm, MS Fowler, K Healy, AL Jackson, M Lurgi, D McClean, NE O'Connor, EJ O'Gorman, and Q Yang (Sept. 2016). Navigating the complexity of ecological stability. en. *Ecology Letters* 19. Ed. by Adler F, 1172–1185. ISSN: 1461023X. https://doi.org/10.1111/ele.12648.

Grilli J, M Adorisio, S Suweis, G Barabás, JR Banavar, S Allesina, and A Maritan (Apr. 2017). Feasibility and coexistence of large ecological communities. en. *Nature Communications* 8, 14389. ISSN: 2041-1723. https://doi.org/10.1038/ncomms14389.

Hale KRS, FS Valdovinos, and ND Martinez (May 2020). Mutualism increases diversity, stability, and function of multiplex networks that integrate pollinators into food webs. *Nature Communications* 11, 2182. ISSN: 2041-1723. https://doi.org/10.1038/s41467-020-15688-w.

Hastings A (Dec. 1980). Disturbance, coexistence, history, and competition for space. en. *Theoretical Population Biology* 18, 363–373. ISSN: 00405809. https://doi.org/10.1016/0040-5809(80)90059-3.

Hutchinson GE (1961). The Paradox of the Plankton. en. *THE AMERICAN NATURALIST*, 9.

Kéfi S, V Domínguez-García, I Donohue, C Fontaine, E Thébault, and V Dakos (Sept. 2019). Advancing our understanding of ecological stability. en. *Ecology Letters* 22. Ed. by Coulson T, 1349–1356. ISSN: 1461-023X, 1461-0248. https://doi.org/10.1111/ele.13340.

Korpelainen H and M Pietiläinen (Dec. 2020). Sorrel (Rumex acetosa L.): Not Only a Weed but a Promising Vegetable and Medicinal Plant. *The Botanical Review* 86, 234–246. ISSN: 1874-9372. https://doi.org/10.1007/s12229-020-09225-z.

Lepori VJ, N Loeuille, and RP Rohr (2022). Robustness vs productivity during evolutionary community assembly: short-term synergies and long-term trade-offs. *bioRxiv*. Publisher: Cold Spring Harbor Laboratory _eprint: https://www.biorxiv.org/content/early/2022/10/18/2022.10.14.512255.full.pdf. https://doi.org/10.1101/2022.10.14.512255.

Levins R (1968). *Evolution in Changing Environments: Some Theoretical Explorations*. Princeton University Press. ISBN: 0-691-07959-5.

Loreau M and C de Mazancourt (May 2013). Biodiversity and ecosystem stability: a synthesis of underlying mechanisms. en. *Ecology Letters* 16. Ed. by Duffy E, 106–115. ISSN: 1461023X. https://doi.org/10.1111/ele.12073.

Lurgi M, D Montoya, and JM Montoya (Feb. 2016). The effects of space and diversity of interaction types on the stability of complex ecological networks. en. *Theoretical Ecology* 9, 3–13. ISSN: 1874-1746. https://doi.org/10.1007/s12080-015-0264-x.

Mccann K, A Hastings, and G Huxel (Oct. 1998). Weak Trophic Interactions and the Balance of Nature. *Nature* 395, 794–798. https://doi.org/10.1038/27427.

Medeiros LP, C Song, and S Saavedra (Sept. 2021). Merging dynamical and structural indicators to measure resilience in multispecies systems. en. *Journal of Animal Ecology* 90, 2027–2040. ISSN: 0021-8790, 1365-2656. https://doi.org/10.1111/1365-2656.13421.

Meszéna G, M Gyllenberg, L Pásztor, and JA Metz (2006). Competitive exclusion and limiting similarity: A unified theory. *Theoretical Population Biology* 69, 68–87. ISSN: 0040-5809. https://doi.org/https://doi.org/10.1016/j.tpb.2005.07.001.

Otto SB, BC Rall, and U Brose (Dec. 2007). Allometric degree distributions facilitate food-web stability. eng. *Nature* 450, 1226–1229. ISSN: 1476-4687. https://doi.org/10.1038/nature06359.

Radchuk V, FD Laender, JS Cabral, I Boulangeat, M Crawford, F Bohn, JD Raedt, C Scherer, JC Svenning, K Thonicke, FM Schurr, V Grimm, and S Kramer-Schadt (Apr. 2019). The dimensionality of stability depends on

disturbance type. en. *Ecology Letters* 22. Ed. by Donohue I, 674–684. ISSN: 1461023X. https://doi.org/10.1111/ele.13226.

Ribando JM (Oct. 2006). Measuring Solid Angles Beyond Dimension Three. en. *Discrete & Computational Geometry* 36, 479–487. ISSN: 0179-5376, 1432-0444. https://doi.org/10.1007/s00454-006-1253-4.

Rohr RP, S Saavedra, and J Bascompte (July 2014). On the structural stability of mutualistic systems. en. *Science* 345, 1253497. ISSN: 0036-8075, 1095-9203. https://doi.org/10.1126/science.1253497.

Rohr RP, S Saavedra, G Peralta, CM Frost, LF Bersier, J Bascompte, and JM Tylianakis (2016). Persist or Produce: A Community Trade-Off Tuned by Species Evenness. *The American Naturalist* 188. PMID: 27622875, 411–422. https://doi.org/10.1086/688046. eprint: https://doi.org/10.1086/688046.

Roughgarden J (1975). A Simple Model for Population Dynamics in Stochastic Environments. *The American Naturalist* 109, 713–736. ISSN: 00030147, 15375323.

Saavedra S, RP Rohr, J Bascompte, O Godoy, NJB Kraft, and JM Levine (Aug. 2017). A structural approach for understanding multispecies coexistence. en. *Ecological Monographs* 87, 470–486. ISSN: 0012-9615, 1557-7015. https://doi.org/10.1002/ecm.1263.

Serván CA, JA Capitán, J Grilli, KE Morrison, and S Allesina (Aug. 2018). Coexistence of many species in random ecosystems. en. *Nature Ecology & Evolution* 2. Number: 8 Publisher: Nature Publishing Group, 1237–1242. ISSN: 2397-334X. https://doi.org/10.1038/s41559-018-0603-6.

Song C, F Altermatt, I Pearse, and S Saavedra (Aug. 2018). Structural changes within trophic levels are constrained by within-family assembly rules at lower trophic levels. en. *Ecology Letters* 21. Ed. by Gomez JM, 1221–1228. ISSN: 1461023X. https://doi.org/10.1111/ele.13091.

Song C, RP Rohr, and S Saavedra (Aug. 2018). A guideline to study the feasibility domain of multi-trophic and changing ecological communities. en. *Journal of Theoretical Biology* 450, 30–36. ISSN: 00225193. https://doi.org/10.1016/j.jtbi.2018.04.030.

Song C, BI Simmons, MJ Fortin, A Gonzalez, CN Kaiser-Bunbury, and S Saavedra (May 2023). Rapid monitoring of ecological persistence. *Proceedings of the National Academy of Sciences* 120. Publisher: Proceedings of the National Academy of Sciences, e2211288120. https://doi.org/10.1073/pnas.2211288120.

Tabi A, F Pennekamp, F Altermatt, R Alther, E Fronhofer, K Horgan, E Mächler, M Pontarp, OL Petchey, and S Saavedra (June 2020). Species multidimensional effects explain idiosyncratic responses of communities to environmental change. *Nature Ecology & Evolution* 4, 1036–1043. https://doi.org/10.1038/s41559-020-1206-6.

Vallina SM and C Le Quéré (Mar. 2011). Stability of complex food webs: Resilience, resistance and the average interaction strength. en. *Journal of Theoretical Biology* 272, 160–173. ISSN: 0022-5193. https://doi.org/10.1016/j.jtbi.2010.11.043.

Van Ruijven J and F Berendse (2009). Long-term persistence of a positive plant diversity–productivity relationship in the absence of legumes. en. *Oikos* 118. _eprint: https://onlinelibrary.wiley.com/doi/pdf/10.1111/j.1600-0706.2008.17119.x, 101–106. ISSN: 1600-0706. https://doi.org/10.1111/j.1600-0706.2008.17119.x.

Volterra V (Oct. 1926). Fluctuations in the Abundance of a Species considered Mathematically1. *Nature* 118, 558–560. ISSN: 0028-0836, 1476-4687. https://doi.org/10.1038/118558a0.

Wainwright CE, TL Staples, LS Charles, TC Flanagan, HR Lai, X Loy, VA Reynolds, and MM Mayfield (Mar. 2018). Links between community ecology theory and ecological restoration are on the rise. en. *Journal of Applied Ecology* 55. Publisher: John Wiley & Sons, Ltd, 570–581. ISSN: 1365-2664. https://doi.org/10.1111/1365-2664.12975.

Williams RJ (Sept. 2008). Effects of network and dynamical model structure on species persistence in large model food webs. en. *Theoretical Ecology* 1, 141–151. ISSN: 1874-1738, 1874-1746. https://doi.org/10.1007/s12080-008-0013-5.

Appendices

0.1 Relation between Ω, D and D_*

In this study, we highlight the importance of taking into account the shape of the feasibility domain and its size to characterize the robustness of coexistence induced by species interactions. Two different measures, therefore, emerge: Ω, a proxy for the probability of coexistence, and D (or D_*), a proxy for the robustness of coexistence. However, these are not independent. Fig. 6 shows the relationship between the two values.

Figure 6. Relation between D and $\Omega^{2/S}$ for random matrices of size S x S. If D controls the distribution of distance to the edge of feasibility, Ω corresponds to a relative volume of the feasibility domain. The two notions are not equivalent, but still are closely related, which is seen here by comparing D to $\Omega^{2/S}$.

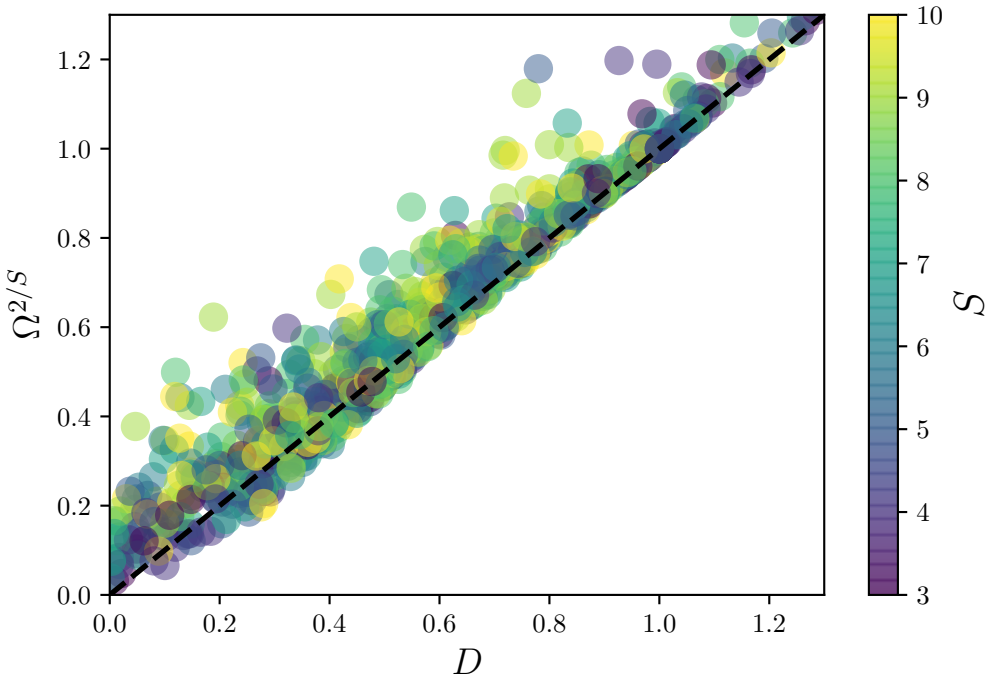

Interestingly, D and D_* are also very closely related. This is somewhat visible in their respective expressions, and confirmed numerically (see Fig. 6). This a useful thing to note because D_* is much simpler to compute, interpret, and manipulate than D, although it is the latter that is expected to driver of the major part of the function $p(\hat{z})$, at least when considering species-rich communities.

0.2 Role of absolute interaction strenght in contribution to vulnerability

Although in the article we used the SCV_i and $r_i/D*$ measures relative to their average in the community, it is also possible to use and compare them in absolute terms. By doing this, a strong correlation between these two values can be observed (Fig. 8). This suggests that species that are constrained by others (through competition, highlighted in red in Fig. 8) are generally the ones that contribute significantly to the overall vulnerability of coexistence. Conversely, species that tend to benefit from others (through facilitation, highlighted in green in Fig. 8) are those that contribute less to the vulnerability of the coexistence of the community.

Figure 7. Correlation between robustness of coexistence D and characteristic distance D_*. Left panel shows this correlation for randomly generated matrices of variable size (S between 3 and 11). The right panel shows this correlation for matrices from real communities (S=4), based on the Barbier et al. (2021) dataset (see section "Application to data from grassland experiment"). The diagonal blue line corresponds to the x=y line in both cases. Note that D and D* are indeed closely related, for random matrices as for empirical matrices.

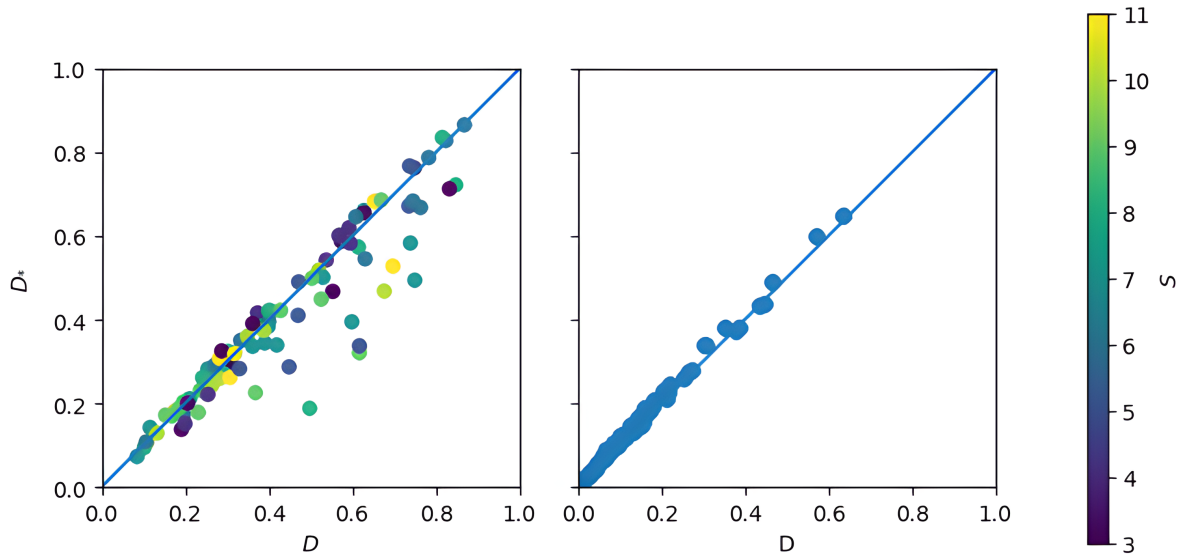
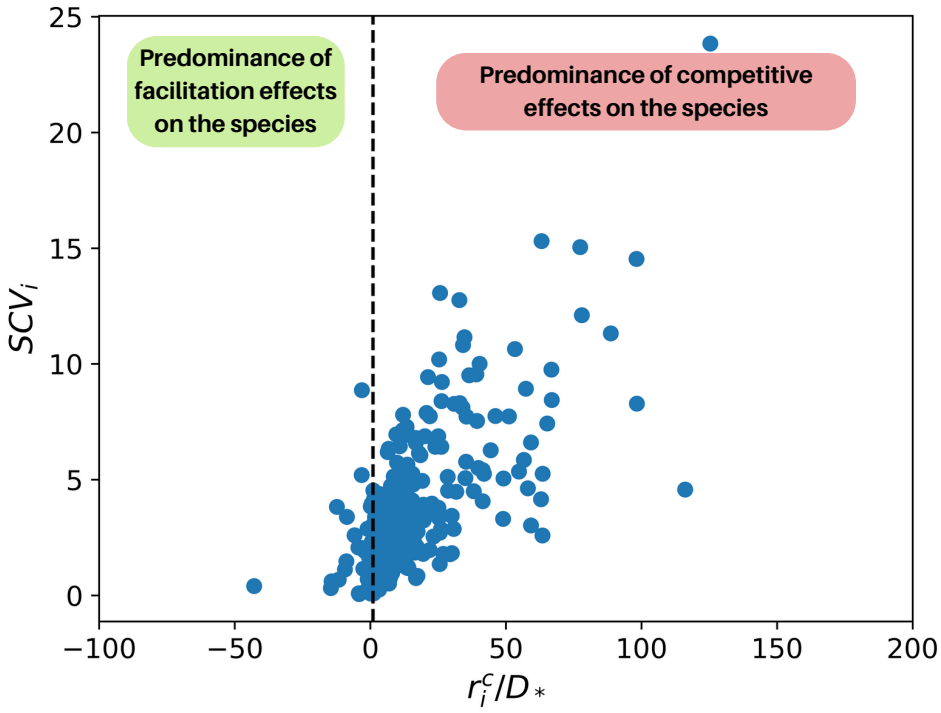
Figure 8. Correlation between the contribution to the vulnerability of each species within a community (SCV$_i$) and the effect of the biotic environment (interaction between species) on each (r_i^c/D_*). Each point represents one species within a community of 10 species (500 points in total). The contribution to the vulnerability of each species is calculated on the basis of equation 11. The vertical dot line corresponds to x=1, the qualitative threshold of the biotic effect on species. If this value is less than 1 (green box on the figure), this implies that the biotic environment is overall favorable (facilitating) to the concerned species. If upper than 1 (red box on the figure), it implies that the biotic environment is overall unfavorable through competition subjected to the species. Spearman rank correlation = 0.67 ; associated p-value : $2.5e^{-68}$